J. Fluid Mech. (1988), *vol.* 194, *pp.* 309–331
Printed in Great Britain

Deflection of a stream of liquid metal by means of an alternating magnetic field

By J. ETAY†, A. J. MESTEL‡ AND H. K. MOFFATT‡

†MADYLAM, B.P. 95, 38400 St. Martin d'Heres Cedex, France

‡Department of Applied Mathematics and Theoretical Physics, University of Cambridge, Silver Street, Cambridge CB3 9EW, UK

(Received 3 December 1987)

When coils carrying high-frequency currents are placed in the neighbourhood of a stream of liquid metal (or other electrically conducting fluid), the magnetic pressure on the liquid surface causes a deflection of the stream. This effect is studied for a two-dimensional stream on the assumptions that the width of the stream is small compared with the scale characterizing the applied magnetic pressure distribution, and that the effect of gravity may be neglected over this scale. The relationship between the angle of deflection of the stream and the power supplied to the perturbing currents is determined. More complex deformations associated with distributed current sources are considered. Experiments are performed in which a thin sheet of mercury is deflected by two antiparallel line currents. The agreement between theory and experiment is reasonable, despite a tendency towards three-dimensionality in the latter. A second configuration is considered in which a thin current-carrying circular jet is deflected by a vertical line current. The path of the deflected jet is calculated. The limitations of the analysis are briefly discussed.

1. Introduction

For many purposes involving the processing of liquid metals, it may be desirable to be able to deflect a stream through a given angle, as indicated in figure 1. In this paper we address the question of whether (and how) such deflection can be achieved by the action of the magnetic pressure p_M associated with a high-frequency magnetic field produced by current sources outside the liquid stream. A high frequency is obviously desirable so that the magnetic field is shielded from the interior of the stream by the skin effect, thus maximizing the effect of magnetic pressure over the liquid surface.

Although the deflecting effect may be physically clear, it is mathematically quite complex to describe, because the magnetic field distribution is itself affected by the (*a priori*) unknown position of the fluid boundary. In order to analyse the effect, we shall therefore make certain simplifying assumptions, as follows:

(1) We confine ourselves to a two-dimensional configuration, in which a sheet of metal, of initial thickness d_0 and uniform velocity u_0, moves under the influence of alternating line currents. Such sheets are used in industrial processes such as the manufacture of metallic ribbon.

(2) We assume that the field frequency, $\omega/2\pi$ is sufficiently high for it to be

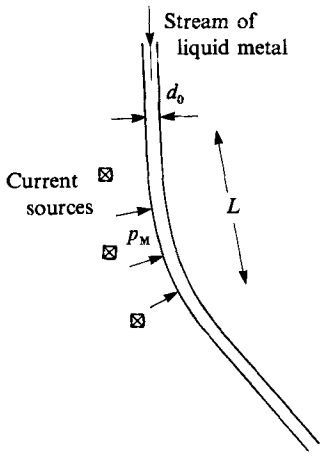

FIGURE 1. Schematic illustration of deflection of liquid metal stream by the magnetic pressure due to high-frequency current sources.

reasonable to treat the effect of the fields entirely in terms of the magnetic pressure on the liquid surface. This requires that the magnetic skin thickness

$$\delta = \left(\frac{2}{\mu_0 \sigma \omega}\right)^{\frac{1}{2}} \tag{1.1}$$

(where σ is the electrical conductivity of the liquid and $\mu_0 = 4\pi \times 10^{-7}$ in SI units) be small compared with the undisturbed thickness of the stream:

$$\tfrac{1}{2}\delta \ll d_0. \tag{1.2}$$

The factor of $\frac{1}{2}$ is included in (1.2) because the magnetic pressure is quadratic in the magnetic field and thus decays twice as quickly.

(3) We assume that d_0 is small compared with the scale L characterizing the distribution of magnetic pressure over the surface, a scale determined by the distribution of the current sources, their distance from the liquid surface and the surface curvature:

$$d_0 \ll L. \tag{1.3}$$

(4) Finally, we assume that gravity may be neglected at least over the scale L on which the deflection takes place. In terms of the upstream velocity u_0 the lengthscale on which gravity acts is

$$l_g = u_0^2/g. \tag{1.4}$$

Hence, we require that

$$L \ll l_g. \tag{1.5}$$

The assumptions (1.2), (1.3) and (1.5) are obviously very restrictive, but they permit significant progress to be made as described in §§2–4 below. The limitations of the analysis will be considered in §5. In §6 we describe experimental deflection of a thin sheet of mercury, and compare the results with theory in §7.

An alternative mechanism for stream deflection is investigated in §8. A current is made to flow along a thin, circular metal jet which is then deflected by interaction with an opposite line current. The assumptions (1.3) and (1.5) are still necessary for analytical progress, but the prohibitive restriction on frequency (1.2) can be relaxed. Indeed, this method can be used even with direct currents. Finally, we conclude in §9.

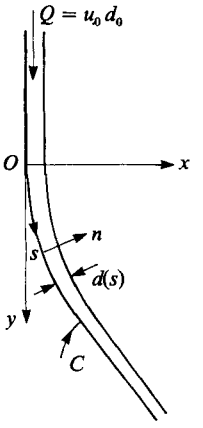

FIGURE 2. The coordinate system.

2. Quasi-one-dimensional analysis

The assumption (1.3) above allows the use of a quasi-one-dimensional analysis, in which the liquid stream is in effect located by the position of its lower (or left-hand) boundary. This is a curve C with parametric equations

$$x = x(s), \quad y = y(s), \tag{2.1}$$

where s represents arclength along C from some fixed point O (as in figure 2). Although gravity is neglected we shall describe x and y as horizontal and vertical coordinates respectively. The stream is also described by its thickness $d(s)$, which is clearly (weakly) non-uniform when deflection occurs. We suppose that, upstream of the region of magnetic influence, conditions are uniform, i.e. the stream has uniform velocity u_0 and thickness d_0 so that the volume flux is

$$Q = u_0 d_0. \tag{2.2}$$

As viscous effects are negligible, the flow is then irrotational everywhere by virtue of the assumption (1.2) which ensures that the sole effect of the magnetic field is to provide a magnetic pressure distribution over the liquid surface.

Let (s, n) be taken as coordinates tangent and normal to C, as in figure 2, and let $u(s, n)$ be the velocity (effectively parallel to C) within the stream. To leading order in the small parameter d_0/L, the component of the equation of motion (the steady Euler equation) in the n-direction is

$$\frac{\partial p}{\partial n} = -\rho u^2 K(s), \tag{2.3}$$

where ρ is the liquid density, p the pressure, and $K(s)$ is the curvature of C at position s. The curvature K is defined to be positive when the surface curves in the direction of $n > 0$, as in figure 2. To the same approximation, the appropriate boundary condition on the upper (or right-hand) boundary is

$$p(s, d_0) = p_0 - \gamma K, \tag{2.4}$$

where p_0 is atmospheric pressure, and γ is the surface tension. On the lower (left-hand) boundary the condition is

$$p(s, 0) = p_0 + p_M + \gamma K, \tag{2.5}$$

where $p_M(s)$ is the magnetic pressure. In writing (2.4) and (2.5) we have assumed that all the driving currents occur on the left-hand side of C. From (2.3) we see that cross-stream variations in the pressure are of order d_0/L. Thus Bernoulli's theorem,

$$p+\tfrac{1}{2}\rho u^2 = p_0+\tfrac{1}{2}\rho u_0^2, \tag{2.6}$$

implies that the velocity in the stream is constant to leading order

$$u = u_0+O\left(\frac{d_0}{L}\right). \tag{2.7}$$

Integrating (2.3) using (2.7) and (2.4) we get

$$p(s,n) = p_0-\gamma K+\rho u_0^2 K(d_0-n) \tag{2.8}$$

and hence the required magnetic pressure $p_M(s)$ is given by

$$p_M = \rho u_0^2 d_0 K(s)\lambda, \tag{2.9}$$

where

$$\lambda = 1-\frac{2\gamma}{\rho u_0^2 d_0}. \tag{2.10}$$

The perturbation to the velocity $u(s,n)$ and width $d(s)$ are now easily determined from Bernoulli's theorem and mass conservation. First, from (2.6) and (2.8), we have

$$u = u_0+K\left[\frac{\gamma}{\rho u_0}-u_0(d_0-n)\right]. \tag{2.11}$$

The flow rate, Q, is constant provided

$$Q = \int_0^{d(s)} u\,\mathrm{d}n = u_0 d-\tfrac{1}{2}K u_0 d_0^2\lambda, \tag{2.12}$$

and so the stream thickness, d, is given by

$$d(s) = d_0+\tfrac{1}{2}K d_0^2\lambda. \tag{2.13}$$

It is clear from the form of (2.10) that the inertia of the uniform stream acts somewhat like a negative surface tension. As the magnetic pressure is positive, the direction in which the stream is deflected (as characterized by the sign of K) may be seen from (2.9) to depend on the sign of λ. We are mainly concerned here with parameter values such that λ is positive, i.e. when the magnetic pressure generates a momentum flux away from the currents. When $\lambda < 0$, the magnetic pressure is strongly resisted by surface tension, with the momentum flux being less important. In both these cases the jet thickness, d, increases during the interaction with the magnetic field. It is of interest to note that when $\lambda = 0$ there is no equilibrium unless the magnetic pressure vanishes. When both λ and p_M are zero, then to lowest order in the jet thickness, any shape C gives rise to an admissible steady state. Somewhat curiously, the path of the stream is maintained by its own surface tension. An analogy can be drawn with Rayleigh's observation (1894) that an arbitrarily shaped one-dimensional string of density ρ per unit length, under a tension T may move tangentially to itself with speed c provided $T = \rho c^2$.

The results (2.9), (2.11) and (2.13) are correct to order $(d_0 K_m)$, where K_m is the maximum value of $K(s)$. The analysis may be extended to higher orders of $(d_0 K_m)$ if

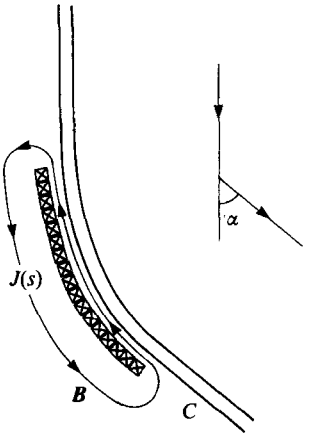

FIGURE 3. Current-sheet configuration giving rise to a desired stream deflection.

some care is taken. Equation (2.3) still holds at the next order provided (2.11) is used for the value of u and that some account is taken of the variation in streamline curvature across the metal stream. If we write

$$K'(s) = d_0 \frac{\partial K}{\partial n}(s, 0) \tag{2.14}$$

then the required value of p_{M}, correct to order $(d_0 K_{\mathrm{m}})^2$, is

$$p_{\mathrm{M}} = \rho u_0^2 d_0 \lambda[K - \tfrac{1}{2}K^2 d_0 + \tfrac{1}{2}K']. \tag{2.15}$$

Now to lowest order, $K' = K^2 d_0$. We thus see that (2.9) is, in fact, correct to order $(K_{\mathrm{m}} d_0)^2$. Second-order corrections to the sheet thickness and tangential velocity may be found from substitution in (2.6) and then using (2.12) as previously. At higher orders, however, the normal component of velocity cannot be ignored and (2.3) breaks down.

The equation (2.9) defines a highly nonlinear relation between the curve C and the external current distribution. We may now formulate two problems: Firstly, for a given distribution of current lines what shape does the metal adopt? Alternatively, if we have a desired path C for the metal stream, how can we arrange the currents so that this is achieved? A problem of the former type was solved numerically using the hodograph method by Shercliff (1981) in his work on the shaping of liquid metal columns (Etay 1980). In that problem the balance is between surface tension and magnetic pressure, corresponding to λ negative. Here we shall consider the inverse problem, and ask: what distribution of external currents can produce a magnetic field which will provide just the magnetic pressure $p_{\mathrm{M}}(s)$ given by (2.9) to yield the required deflection? One possible solution (and there will be many others) is provided by placing coils so as (in effect) to provide a current sheet $J(s)\cos\omega t$ near to the deflected stream, as indicated in figure 3. (To achieve this configuration in practice would require continuous adjustment of the position of the coils as the required deflection of the stream is produced.) This current sheet produces a magnetic field $B(s)\cos\omega t$ in the gap between the coils and the stream where

$$B(s) = \mu_0 J(s). \tag{2.16}$$

This field is effectively parallel to C, and provides a time-averaged magnetic pressure

$$p_{\mathrm{M}} = \tfrac{1}{4}\mu_0 B^2 = \tfrac{1}{4}\mu_0 J^2. \tag{2.17}$$

Hence the required magnetic pressure (2.9) is achieved provided

$$\mu_0 J^2 = 4\rho u_0^2 \lambda K d_0 + O(K_{\mathrm{m}} d_0)^3. \tag{2.18}$$

The strategy therefore appears straightforward: first describe the required curve C in terms of its curvature $K(s)$; then engineer the coils and electromagnetic controls so that a current amplitude $J(s)$ satisfying (2.18) is provided. The required deflection of the stream can then be maintained.

If we use the expression $K = \mathrm{d}\psi/\mathrm{d}s$, where ψ is the angle that the tangent to C makes with the horizontal, then by integrating (2.18) we obtain the result

$$4\rho u_0^2 d_0 \lambda \alpha = \int_C \mu_0 J^2 \,\mathrm{d}s = \int_C \frac{B^2}{\mu_0}\mathrm{d}s, \tag{2.19}$$

where α is the total angle of deflection of the stream. We may express α in terms of the power supplied to the coils (per unit length in the z-direction). This power, W, is balanced by the Joule heating in the metal stream

$$W = \int \frac{|\boldsymbol{\nabla} \wedge \boldsymbol{B}|^2}{\mu_0^2 \sigma}\mathrm{d}V \tag{2.20}$$

or, in terms of the skin depth approximation,

$$W = \frac{1}{\mu_0^2 \sigma \delta^2}\int_0^\infty \mathrm{e}^{-2n/\delta}\mathrm{d}n \int_C B^2(s)\,\mathrm{d}s = \tfrac{1}{4}\delta\omega \int_C \frac{B^2}{\mu_0}\mathrm{d}s. \tag{2.21}$$

Together (2.19) and (2.21) give a simple relationship between the angle of deflection and the power supplied to the external coils,

$$\alpha = \frac{W/\omega\delta}{\rho u_0^2 d_0 \lambda}. \tag{2.22}$$

Recalling the definition of δ in (1.1), we can see that the power needed to obtain a given deflection α behaves as $\omega^{\frac{1}{2}}$, provided the frequency ω is sufficiently large that the skin-depth approximation applies. Thus, in practice there will exist some optimal frequency at which the deflection effect is still pronounced, but for which the power dissipated in the metal is relatively low. This optimum value will probably occur when

$$\delta \sim d_0. \tag{2.23}$$

3. Deflecting action of a weak line current

If the current sources are fixed *ab initio*, then the problem is much more complicated, because the magnetic-field distribution is strongly coupled with the stream deflection. If the sources are weak, however, then the deflection will also be weak, and some progress is possible by perturbation analysis. We illustrate this with reference to the action of a concentrated line current $I\cos\omega t$ placed at a distance L from a stream $Q = u_0 d_0$ (figure 4). When $I = 0$ the position of the stream is $0 < x < d_0$. When $I \neq 0$, we suppose that the stream is symmetrically perturbed as indicated in the figure. To leading order, however, the magnetic-field distribution

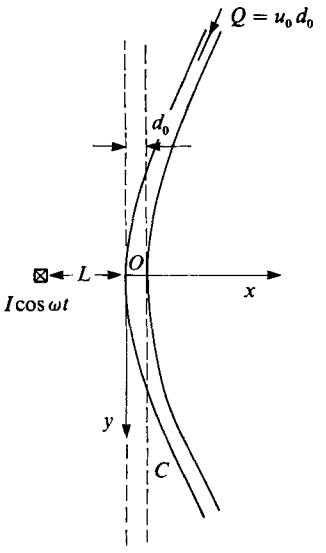

FIGURE 4. Stream deflection by a concentrated current source. For a weak current, the shape of C is given by (3.6).

may still be calculated as if the stream were in the undisturbed position. There is then an image current $-I\cos\omega t$ at $x = L$, $y = 0$, and the net magnetic field on $x = 0$, is $\boldsymbol{B} = (0, B_y, 0)$ where

$$B_y = \frac{\mu_0 I}{\pi}\frac{L}{L^2+y^2}\cos\omega t. \tag{3.1}$$

The resulting magnetic pressure is

$$p_{\mathrm{M}} = \frac{\mu_0 L^2 I^2}{4\pi^2}\frac{1}{(L^2+y^2)^2} \tag{3.2}$$

and the deflection of the surface, from (2.9) with $K \sim \mathrm{d}^2x/\mathrm{d}y^2$, is given by

$$\frac{\mathrm{d}^2x}{\mathrm{d}y^2} = \frac{N}{4\pi^2}\frac{L^3}{(L^2+y^2)^2}, \tag{3.3}$$

where the magnetic interaction parameter, N, is given by

$$N = \frac{\mu_0 I^2}{\rho u_0^2 d_0 L\lambda}. \tag{3.4}$$

We integrate this with 'initial' conditions

$$x(0) = \frac{\mathrm{d}x}{\mathrm{d}y}(0) = 0 \tag{3.5}$$

with the result

$$x(y) = \frac{N}{8\pi^2}\, y\tan^{-1}\frac{y}{L}, \tag{3.6}$$

an even function of y, as expected. When $|y| \gg L$, this gives

$$x = \frac{N}{16\pi}|y| \tag{3.7}$$

so that the net angle of deflection is given by

$$\alpha = \frac{N}{8\pi}. \tag{3.8}$$

Equation (3.8) is strictly valid only provided the deflection is weak, i.e. $\alpha \ll 1$; however the results of §2 suggest that here also an arbitrarily large deflection of the stream may be achieved if the dimensionless parameter N is increased to a sufficiently large value. This parameter may be regarded as the magnetic interaction parameter, giving a measure of the transverse flux of momentum generated by the magnetic forces relative to the flux of momentum $\rho u_0^2 d_0$ in the incoming stream.

The magnetic-field lines of a line current and its image consist of a family of coaxial circles. Thus, the analysis of this section and the result (3.8) in particular may be extended to the more realistic case when the line current is replaced by a wire of finite, circular cross-section. Let the wire consist of a circular cylinder radius r whose axis lies on $x = -b, y = 0$. At high frequency, the current in the wire flows near the surface and is equivalent to a line current at $x = -L, y = 0$, where

$$L^2 = b^2 - r^2. \tag{3.9}$$

For this value of L, the deflection obtained is given by (3.8) with (3.4). It should be noted that no such exact result holds for low frequencies (or d.c.). The surface of the wire must be a magnetic-field line for (3.9) to hold.

4. More complex deformation

In the experiments that follow we shall use for electrical convenience a device which may be modelled by two opposite line currents a fixed distance, a, apart. It is a simple matter to extend the theory of §3 to include this case. The magnetic field may be represented as a sum of two terms similar to (3.1) which can then be squared and integrated to calculate the deflection angle α. When the two line currents lie in a horizontal plane a distance a apart, the result corresponding to (3.8) is

$$\alpha = \frac{N}{8\pi} \frac{a^2}{(L+a)(2L+a)}, \tag{4.1}$$

whereas when they lie in a vertical plane we find

$$\alpha = \frac{N}{8\pi} \frac{2a^2}{a^2+4L^2}. \tag{4.2}$$

Now when $a \gg L$, which is the case of interest in §§6 and 7, (4.2) describes merely a second-order correction. However, there is a more important adjustment that must be made when $a \gg L$ and the line currents are vertical. The 'weak-deflection' approximation assumes that the deviation of the jet from the vertical is small over the entire region of interest. Yet if we consider the effects of each line current independently, it is clear that a deflection angle α due to the upper line current will lead to a separation between the lower line current and the jet of order $a\alpha$ which can be large compared with L. If we treat the line currents as independent, then the total angle of deflection, α_2, is given in terms of that due to a single line current, α_1, by

$$\alpha_2 = \alpha_1 \left(1 + \frac{1}{\cos\alpha_1 + (a/L)\sin\alpha_1}\right). \tag{4.3}$$

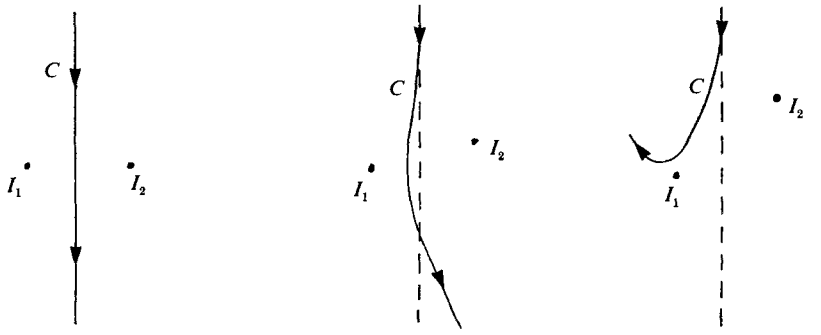

(*a*) (*b*) (*c*)

FIGURE 5. Deflection of a narrow stream by two equal currents I_1 and I_2 for various positions of I_2. The position of I_2 may be used as a sensitive control for the ultimate direction of the stream, gravity being neglected.

So far, we have supposed that the current sources are all placed to one side of the stream. More complex stream deformation may clearly be achieved if current sources on both sides are used. In the present 'thin-stream' approximation, the stream may be represented by a directed curve C. The magnetic field $\boldsymbol{B}$ on either side of the curve is a potential field with appropriate singularities at the current sources, and satisfies

$$\boldsymbol{B}\cdot\hat{\boldsymbol{n}} = 0 \quad \text{on} \quad C, \tag{4.4}$$

with C approached from either side. The form of C is determined by the differential equation (2.9), with the appropriate value of p_{M} being the difference in the magnetic pressures on either side of C. Determination of the curve C therefore involves an unusual coupling of potential theory and differential geometry; physically there seems little doubt that a solution invariably exists, although subsidiary conditions may have to be imposed to guarantee uniqueness. We shall not attempt to pursue in this paper the general analysis, which is likely to require a numerical approach.

To illustrate the possible effects, suppose that we start with a stream passing symmetrically between two equal current sources I_1, I_2 as indicated in figure 5(*a*). Suppose that we now slowly move I_2 upwards (figure 5*b*). The stream then first feels the influence of I_2 and is deflected towards I_1; it is then more strongly influenced by I_1, and is deflected in a net 'south-easterly' direction as indicated in the figure.

If the upward displacement of I_2 is continued (figure 5*c*), then a critical point is reached, beyond which the stream is deflected upwards rather than downwards by I_1. (The thin-stream analysis will be invalid in the immediate neighbourhood of this critical value, but will hold either side of it.) The position of I_2 may thus be used as a sensitive control for the ultimate direction of the stream.

5. Limitations of the analysis

In the introduction we have indicated four simplifying assumptions, all in effect idealizations. We now consider the qualitative effects of relaxing these assumptions.

Suppose first that δ is not small compared with d_0, so that the field penetrates a significant distance into the liquid stream. This weakens the magnetic pressure over

the surface, thus tending to diminish the deflecting effect. An additional complication is that the mean Lorentz force within the fluid will in general generate vorticity in the stream, which can thus no longer be treated as irrotational. The problem therefore becomes more complex, although a small-perturbation analysis (analogous to that of §3) will still be possible. If the ratio $\delta/2d_0$ is small but not negligible then, bearing in mind (1.2) and (1.3), a first correction to the analysis may be obtained by replacing the magnetic pressure p_M by

$$p_M(1-e^{-2d_0/\delta}). \tag{5.1}$$

Secondly, if d_0 is not small compared with L, then the quasi-one-dimensional analysis of §2 is no longer justifiable, and a fully two-dimensional analysis would be required to find the position of both boundaries. This problem should be amenable to the variational and/or relaxation techniques of the kind adopted by Sneyd & Moffatt (1982) and Mestel (1982) for the problem of magnetic levitation.

Thirdly, if L is not small compared with the gravitational lengthscale l_g, then the tendency of gravity to resist deflection of the stream from the vertical within the region of magnetic deflection can no longer be neglected. Clearly, behaviour such as that depicted in figure 5(*c*) becomes implausible in such circumstances. Of course, as the stream descends, its speed increases under the influence of gravity (with compensating decrease in width) so that l_g increases, and paradoxically the gravitational effect becomes weaker relative to the magnetic perturbing effects on a fixed scale L.

If all three assumptions (1.2), (1.3) and (1.5) are simultaneously relaxed, then we are faced with a problem of great difficulty, whose solution would require heavy computational methods. Likewise, should our fourth and final assumption of two-dimensionality cease to apply, we would probably have to resort to numerical techniques. We shall see from the experiments described in the next section that the end effects on a nearly two-dimensional sheet are somewhat troublesome. Not only does the three-dimensional nature of surface tension become important, but also the magnetic field becomes hard to calculate near the end regions. Furthermore, the magnetic field is no longer topologically excluded from the far side of the metal stream, and some account of the magnetic pressure there should be taken. In spite of these factors, we shall see that the theory of the preceding sections does give a reasonable description of the stream behaviour.

6. Experiments

Experiments were performed in order to measure the deflection of a nearly two-dimensional stream by line currents. The experimental set-up used is shown in figure 6 and is described in full by Etay & Garnier (1982). Essentially, the facility consists of a mercury-filled hydraulic circuit containing a freely falling column. The initial cross-section of the column is determined by a detachable nozzle, moulded from a two-component resin, whose shape may be chosen at will. The alternating magnetic field is supplied by cooled, insulated copper inductors connected to adjustable capacitors. The circuit is powered by a 100 kW generator and is tuned to resonance.

In these deflection experiments, the chosen nozzle is gently converging ending in a slit 1 mm wide and 39 mm long. The outlet must be carefully cleaned to prevent tearing of the mercury sheet. Photographs, with an exposure time of 10^{-3} s were taken by a camera mounted in the plane perpendicular to the metal sheet. The exact

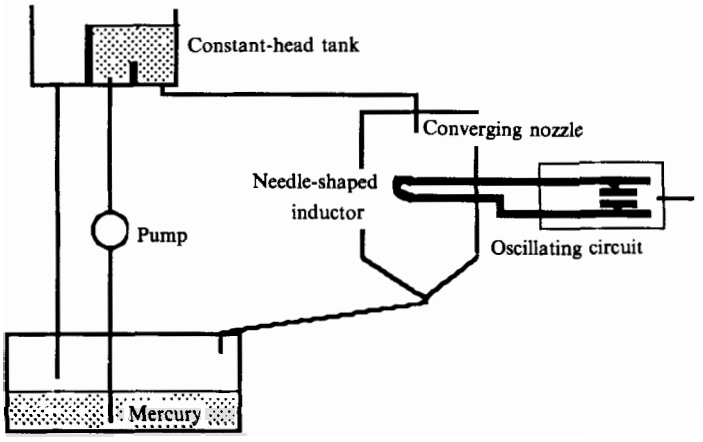

FIGURE 6. The experimental set-up

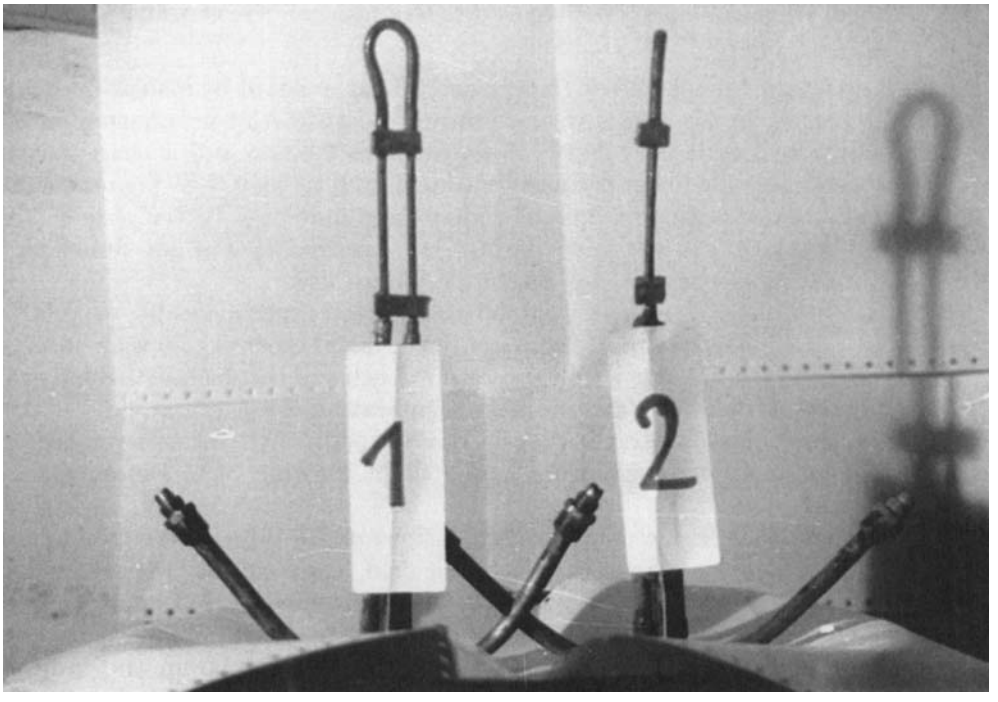

FIGURE 7. The (identical) inductors used in the experiments. Number 1 is horizontal, number 2 is vertical.

position of the camera is adjustable though there is a certain amount of parallax. The deflection angle was measured on the photographs.

The inductors are made from hollow copper tubing of 3–4 mm diameter through which cooling water is passed. A single line current would give rise to a large self-inductance with resultant inconvenience for the tuning capacitor. Instead, two needle-shaped inductors were built for independent use as shown in figure 7. The current flows along one branch of the needle and then returns along the other. In the middle of the inductor the field is approximately that due to two line currents. The

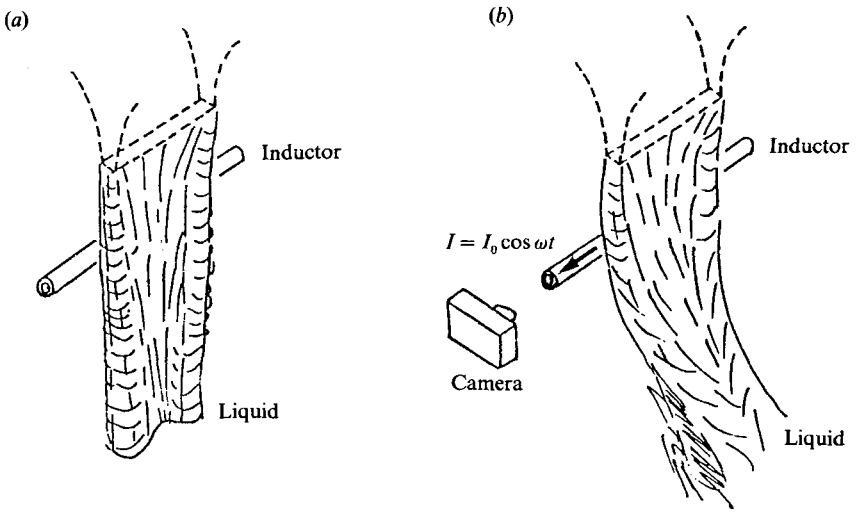

FIGURE 8. Sketch of the development of a nearly two-dimensional stream. (*a*) Without current; (*b*) deflected by a high-frequency line current.

distance between the branch axes is 15 mm, and is held constant by insulating struts. The current flowing in the inductor varies from 0 to 1520 A at a frequency of 350 kHz. The electromagnetic skin depth, δ, is therefore 0.8 mm and a characteristic value of the magnetic field near the sheet varies from 0 to 2000 G. A higher current could not be obtained with this kind of copper-tube inductor. In fact, the cooling power of the pressurized water used during the experiments was not sufficient to prevent overheating of the inductor during prolonged use.

A truly two-dimensional geometry cannot be achieved experimentally, even in the absence of electromagnetic effects. The initially flat metal sheet develops as sketched in figure 8. Surface tension causes rolls to form at both ends of the sheet which grow as the metal falls. Of course, in any industrial application, the sheet would be longer and thus end effects less important than in these experiments. A further departure from two-dimensionality occurs owing to the slight twisting of the sheet when it leaves the nozzle.

When an alternating, high-frequency current flows in the inductor the liquid metal sheet is repelled from the region of high magnetic field. The resulting shape, as we saw in §3, depends mainly on a balance between inertial and Lorentz forces. Unfortunately, the departures from two-dimensionality are amplified by electromagnetic effects. The ends of the sheet are repelled further from the inductor than is the middle, owing to the three-dimensionality of the magnetic field there. The resulting curved cross-section aggravates the tendency of the sheet to contract and its thickness increases. The measurement of the deflection angle can thus become difficult. This effect is illustrated on figure 9 which shows the 'worst' kind of deflection that can occur.

7. Comparison between calculated and experimental results

The dimensionless parameter that controls the deflection is

$$N = \frac{\mu_0 I^2}{\rho u_0^2 d_0 L}, \tag{7.1}$$

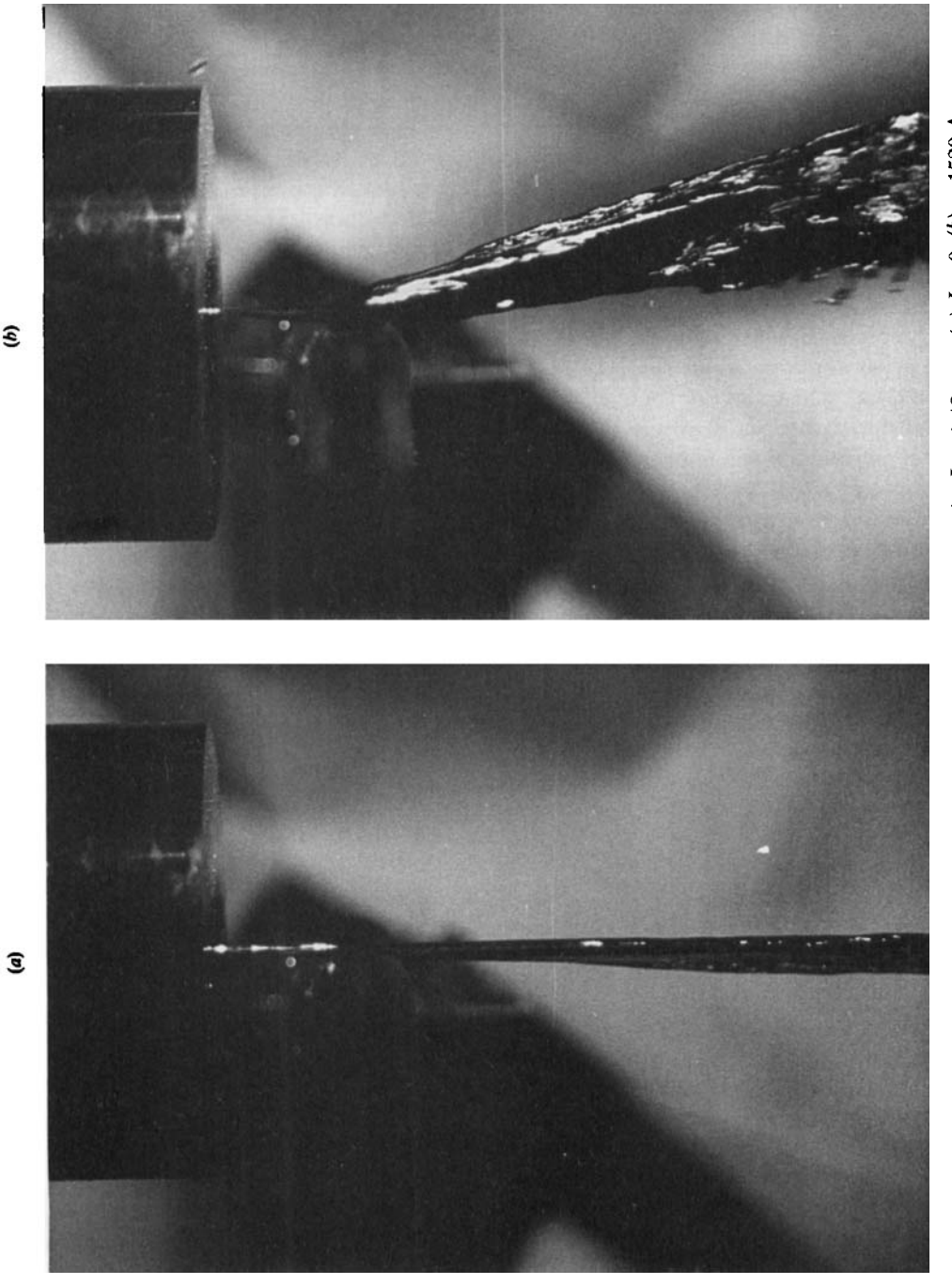

FIGURE 9. Non-uniform deflection of the metal stream: $u_0 = 1.74$ m/s, $L = 1.42$ mm. (*a*) $I = 0$, (*b*) = 1520 A.

where μ_0 is the vacuum permeability and ρ the density of the metal ($4\pi \times 10^{-7}$ and 13.6×10^3 respectively in SI units). The total current flowing in the inductor, I, is measured by an oscilloscope. The sheet thickness, d_0, and the flow velocity, u_0, are taken to be the slit width, and the velocity through the slit as calculated from the measured flow rate. The greatest error in calculating the experimental value of N derives from the estimate of L. In keeping with (3.9), L is defined in terms of b, the distance between the centre of the coil and the liquid stream. The value of b was measured on a photograph taken with a 45° mirror placed below the inductor. If b is small, which is desirable for maximum effect, then the accuracy of this measurement is low. Should b be too small, however, flapping of the stream caused by vibration of the experimental set-up may lead to undesirable contact between the coil and the stream. Moreover, if the coil is not held sufficiently rigid then the repulsion between it and the mercury will cause it to move slightly. In practice, b was taken as the horizontal gap between the coil and the slit.

The three-dimensionality of the deflected jet ensures that the measurement of the deflection angle, α, is not easy. The maximum deflection, $\alpha_{\max}$, occurs at the ends of the sheet, which are deflected in a manner not wholly described by the two-dimensional theory. However the minimum deflection, $\alpha_{\min}$ is underestimated both by the parallax of the photographs and by any adhesion that may occur between the stream and the inductor. A curious feature of the observed deflection was that the stream did not appear to bend until below the position of maximum pressure, whereas theoretically this should occur very slightly above that position. This was probably an observational effect due to the three-dimensionality. Taking the above into account, it was felt best to define α as the average of $\alpha_{\max}$ and $\alpha_{\min}$.

Two sets of experiments were performed, one with the inductor horizontal (so that only one branch of the inductor has a large effect on the stream) and the other with a vertical inductor, so that the stream is deflected by each branch in turn. According to (4.1) and (5.1), when α is not too large it is related to N through the relation

$$\alpha = \frac{N_{\text{hor}}}{8\pi}, \tag{7.2}$$

where

$$N_{\text{hor}} = N \frac{a^2}{(L+a)(2L+a)} (1 - \mathrm{e}^{-2d_0/\delta}) \tag{7.3}$$

when the inductor is horizontal. When it is vertical, we have from (4.2), (4.3) and (5.1)

$$\alpha = \frac{N_{\text{ver}}}{8\pi} \left(1 + \frac{1}{1 + \frac{a}{L} \frac{N_{\text{ver}}}{8\pi}} \right), \tag{7.4}$$

where

$$N_{\text{ver}} = N \frac{a^2}{a^2 + 4L^2} (1 - \mathrm{e}^{-2d_0/\delta}). \tag{7.5}$$

Equation (7.4) defines a deflection angle which is a nonlinear function of N_{ver}. It varies between a value due to deflection by both branches of the inductor in turn, and one where only the uppermost branch is important. In the experiments, a typical value of a/L was about 6, and N was about 10. The deflection was thus noticeably greater when the inductor was vertical.

The experimental values of α (measured in degrees) are plotted in figure 10 as functions of N_{ver} and N_{hor}. The theoretical line (7.2) and curve (7.4) are drawn on the figure for comparison. The agreement is satisfactory for α small, but not surprisingly,

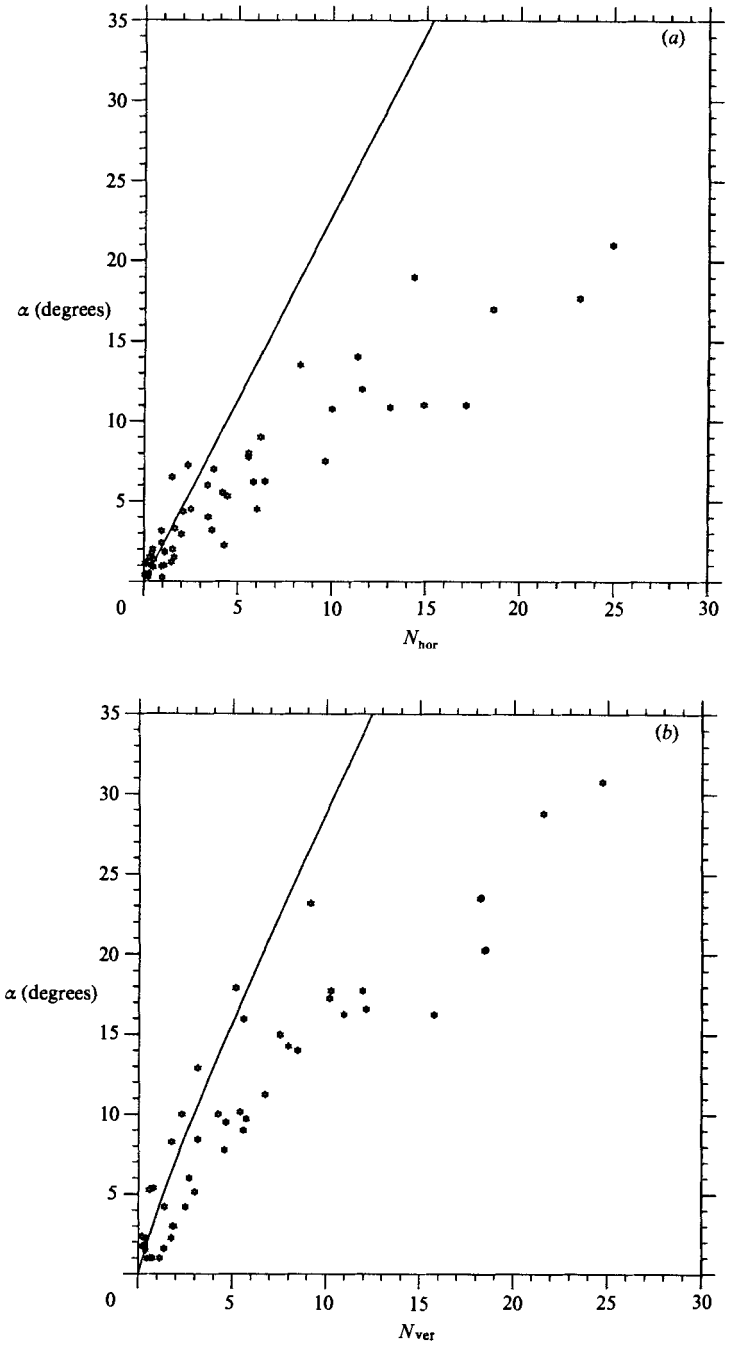

FIGURE 10. Observed deflection angle α (in degrees) against N. (*a*) Horizontal, (*b*) vertical.

the theory overestimates the obtained deflection angle for N (and α) large. The manner in which this occurs appears to be fairly systematic. There are a number of reasons why this might be expected. First, (7.2) and (7.4) apply only when α is small, whereas the experiments cover a wide range of α. The 'weak-deflection' approximation, whereby the magnetic field may be easily calculated, thus breaks down.

Secondly, the constraints (1.2) and (1.3) are only weakly satisfied in the experiments. As a result, the unidirectional irrotational flow assumed in the theory may not be wholly accurate. Thirdly, it is clear that the three-dimensionality of the experiments will lead to a reduced deflection. It also hinders observation of α as we have already discussed. Finally, we should recall the difficulties inherent in the measurement of L. It may well be that there is a systematic underestimation of L when α is appreciably large. Bearing in mind the difficulties inherent in the measurement, it was felt that the agreement between theory and experiment was satisfactory.

8. Deflection of a current-carrying jet

We now turn to a problem that, although related, is characterized by physical mechanisms that are somewhat different. We have seen above that there are some practical difficulties in controlling a stream that is not wholly two-dimensional. In practice one would not choose to transport metal in this manner without a definite reason, as a cylindrical jet would normally be more convenient. However, the method we have described above depends intrinsically on two-dimensionality. A thin cylindrical stream would only be weakly deflected as the magnetic pressure on the far side of the stream would almost balance that on the near side. A further restriction on the use of the above controlling mechanism derives from the constraint (1.2) which requires the skin depth to be small compared with the already thin stream thickness. We might wonder if a way of avoiding these limitations could be devised. One such means exploits the repulsive force that exists between two line currents. If we cause a current to flow along the jet it can be deflected by suitably placed guiding currents. In this section we investigate this phenomenon.

Instead of a thin sheet of metal we consider a thin jet, radius d_0, whose centreline is coplanar with a (vertical) line current, strength I_1, as in figure 11. The top and bottom of the jet we assume to be electrically connected so that a current, $-I_2$, may be induced along the jet. These currents may be either d.c. or a.c. In the former case, it will of course be necessary to apply a potential difference along the metal jet, whereas if the driving current is alternating, we may rely on induction to drive a reverse current I_2. The magnitude of I_2 will then depend in general on the mutual and self-inductances of the circuit geometry. As the position of the jet is unknown *ab initio*, the unknown inductances will lead to complications. However, we may simplify the problem by linking the two circuits with a highly permeable ferromagnetic core. Once the system is energized, the tangential component of $\boldsymbol{B}$ will vanish on the core surface, ensuring that the induced current is equal and opposite to the driving current,

$$I_2 = I_1. \tag{8.1}$$

This configuration, wherein a loop of liquid metal acts as the secondary 'coil' of a transformer, is also used in the design of channel induction furnaces (e.g. Mestel 1984). Equation (8.1) may also hold even when the currents are direct, as from a practical point of view it may well be convenient to join the line current I_1 and the jet in a single circuit. In what follows, we shall not distinguish between the a.c. and d.c. cases and to avoid the appearance of spurious factors of 2, we shall assume that the r.m.s. values are used for alternating currents.

Once again, we describe the metal by means of the parameterized curve C, which now represents the centreline of the (circular) jet. The driving current I_1 occupies the line $x = z = 0$. As compared with the problem studied in §§2–4, the electric currents

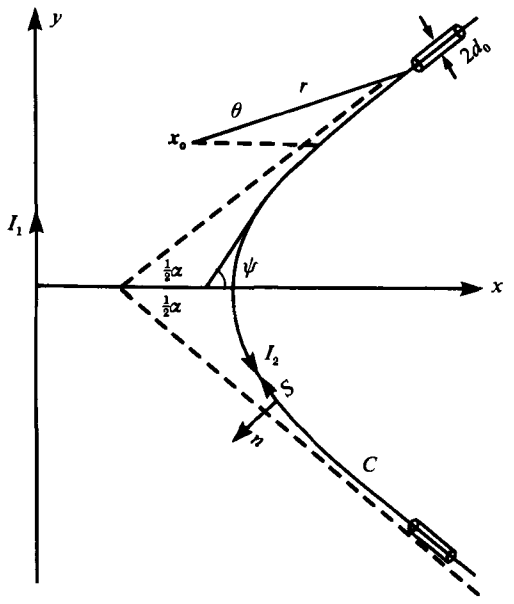

FIGURE 11. Configuration for the deflection of a current-carrying jet.

now lie in the (x, y)-plane, with the magnetic field (locally) in the z-direction, rather than vice versa.

We now consider the force balance on a small portion of the jet. We shall neglect surface tension and assume the cross-sectional area, πd_0^2 and hence the fluid velocity, u_0, are constant. The normal acceleration of the fluid element is provided by the time-averaged electromagnetic forces integrated over the jet cross-section

$$\pi d_0^2 \rho u_0^2 K(s) = \int \boldsymbol{j} \wedge \boldsymbol{B} \cdot \hat{\boldsymbol{n}} \, \mathrm{d}A \tag{8.2}$$

or

$$\pi d_0^2 \rho u_0^2 K(s) = I_2(B_1 + B_2), \tag{8.3}$$

where B_1 is the magnetic field due to the driving current I_1

$$B_1 = \frac{\mu_0 I_1}{2\pi x}, \tag{8.4}$$

and B_2 is the average over the cross-section of the jet of the field due to the circuit involving the jet. This average would be zero if the jet were a perfect right cylinder, but in general has two terms, one due to the local current curvature, and one due to the effects of the distant, non-parallel currents. At a general point in the (x, y)-plane at some distance from the jet, $\boldsymbol{x}_0$, we may find B_2 from the Biot–Savart law and the thin-jet approximation:

$$B_2(\boldsymbol{x}_0) = -\frac{\mu_0 I_2}{4\pi} \int_C \frac{\mathrm{d}\theta}{r(\boldsymbol{x}_0, \theta)}, \tag{8.5}$$

where r and θ are polar coordinates centred on $\boldsymbol{x}_0$, as in figure 11. As $\boldsymbol{x}_0$ approaches C the integrand of (8.5) is singular. This is not surprising, as we are neglecting the finite thickness of the jet. However, even as we perform the average over a tube of radius d_0 around C, we obtain an expression that is logarithmically infinite as

$d_0 \to 0$. This result is related to the fact that the self-inductance of a circular current loop is infinite. When we allow for the finite radius of the jet we obtain the result

$$B_2(s) = -\frac{\mu_0 I_2}{4\pi}\left[K(s)\left(\log\frac{8}{Kd_0} - f\left(\frac{\delta}{d_0}\right)\right) + \oint\frac{\mathrm{d}\theta}{r}\right] + O(Kd_0) \tag{8.6}$$

(see Elliott 1966, p. 314 and Thompson 1962, p. 107). The last term in the square brackets in (8.6) represents a path integral over the jet from which the singularity has been removed. Formally,

$$\oint\frac{\mathrm{d}\theta}{r} = \int_{\psi-\pi}^{\psi}\left(\frac{1}{\mathrm{r}(\mathrm{s},\theta)} - \frac{K(s)}{2\sin(\psi-\theta)}\right)\mathrm{d}\theta, \tag{8.7}$$

where $\psi(s)$ is the angle between C and the x-axis is in figure 11. The term $f(\delta/d_0)$ in (8.6) is a function of frequency, and may be derived from the distribution of current over the cross-section of the jet. It lies between 1 (high frequency, when skin effects dominate) and $\frac{1}{2}$ (low frequency or d.c., when the current is uniform). As Kd_0 is small, the exact value of f is not very important. It should be noted that unlike the process outlined in §§2–4, the configuration described in this section does not require the skin effect and its associated magnetic pressures in order to function. Thus, any value of the frequency is admissible.

From now on, we shall treat the jet as one-dimensional, defined by the curve C. Combining (8.3), (8.4) and (8.6) we obtain

$$Kx = \beta\left(1 - \frac{I_2}{2I_1}x\oint\frac{\mathrm{d}\theta}{r}\right), \tag{8.8}$$

where

$$\beta = \left[\frac{2\pi^2\rho u_0^2 d_0^2}{\mu_0 I_1 I_2} + \frac{I_2}{2I_1}\left(\log\frac{8}{Kd_0} - f\right)\right]^{-1}. \tag{8.9}$$

We may think of β as a modified interaction parameter. As Kd_0 is small, we note that when $I_1 \sim I_2$, β is also small, irrespective of the values of the other parameters. In this case, β is a slowly varying function of the curvature, K. In practice, however, the logarithm may not be too large, and it may be worth considering $O(1)$-values of β. When $I_2 \ll I_1$, however, β may take all values, but is a constant, β_0.

To begin with, we shall consider the latter case. Physically, this amounts to neglecting the field due to the secondary circuit, C. A moment's reflection reveals that in this case the curve C is identical to the path a moving, suitable charged particle would adopt under the influence of the magnetic field $\boldsymbol{B}_1$. Equation (8.8) reduces to

$$Kx = \beta_0 = -x\cos\psi\frac{\mathrm{d}\psi}{\mathrm{d}x} \tag{8.10}$$

and may easily be solved parametrically in terms of the angle ψ between the tangent to C and the x-axis, giving

$$x(\psi) = x_0\,\mathrm{e}^{-\sin\psi/\beta_0}$$

$$y(\psi) = y_0 - \int_0^{\psi}\frac{x_0}{\beta_0}\sin\eta\,\mathrm{e}^{-\sin\eta/\beta_0}\,\mathrm{d}\eta, \tag{8.11}$$

where (x_0, y_0) is the point on C where $\psi = 0$. Equation (8.11) represents an infinite periodic curve which, somewhat amusingly, resembles in shape the electrical symbol for an inductor, as in figure 12.

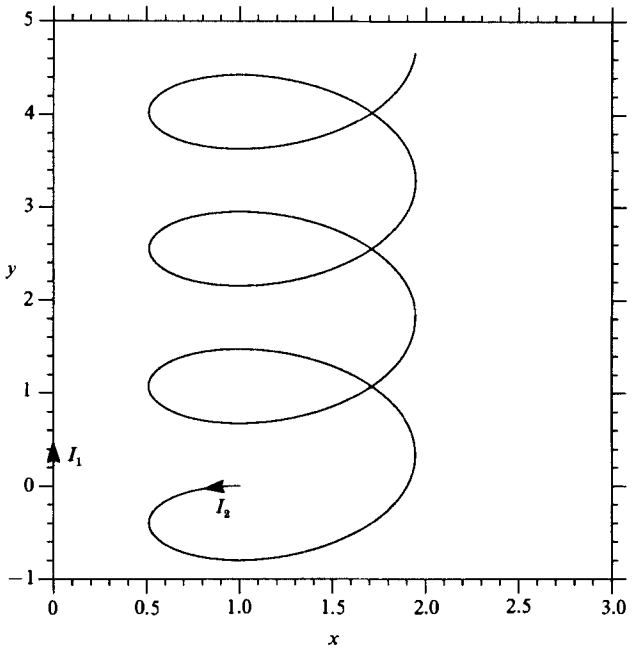

FIGURE 12. Theoretical path of a weak current-carrying jet under the influence of a vertical line current, for $\beta_0 = 1.5$.

The curve defined by (8.11) crosses itself at least once in each period of 2π. Clearly such a crossing is physically inadmissible when C represents a continuous stream of metal. We must consider more precisely the problem to which (8.10) applies. Any equilibrium configuration for the jet, C, must satisfy (8.3) at all points where the jet is free, that is when no external forces act upon it. Now it is clear physically that it will be impossible for the entirety of the closed circuit C to be free, for then C will be repelled *in toto* away from the driving line current. For the circuit C exerts no net force on itself, while it can be shown that the x-component of the total force due to the line current

$$\frac{\mu_0}{2\pi}|I_1 I_2|\oint_C \frac{\hat{\boldsymbol{x}}\cdot \mathrm{d}\boldsymbol{l}}{x} > 0 \tag{8.12}$$

for any closed curve C. Thus, part of C must be held fixed, corresponding to the rigid pipes through which the metal is being pumped. As a result, we are only interested in a portion of the curves defined by (8.11). If the jet is ejected from a nozzle at the point $x(\psi_0), y(\psi_0)$ at an angle ψ_0 to the horizontal and is collected in a bath at say $y = y_b$, we would expect solutions of the form (8.11) to exist, for some parameter ranges. In figure 13, we show some of the curves defined by (8.11) drawn for $0 < \psi < \pi$, corresponding to a jet approaching horizontally and being deflected through 180°. For values of ψ outside this range the jet would be attracted by the line current rather than repelled, but the solution would remain valid until it crossed itself. The curves are normalized so that $\psi = 0$ at $x = 1$, $\psi = \frac{1}{2}\pi$ at $y = 0$, and are drawn for differing values of β_0. The actual jet may occupy any portion of the curve corresponding to an appropriate value of β_0.

For large β_0, the curves are almost circular. This is to be expected, as large β_0 corresponds to a high accelerating Lorentz force for a given jet velocity, and thus a

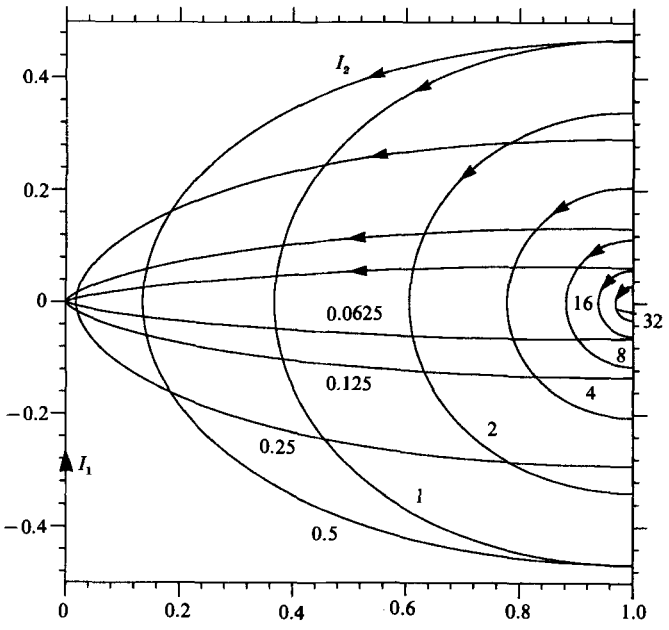

FIGURE 13. Possible jet paths suitably normalized. $\beta_0 = 0.0625, 0.125, 0.25, 0.5, 1, 2, 4, 8, 16, 32$.

small radius of curvature for C. This implies that the driving magnetic field, $\boldsymbol{B}_1$, will not vary greatly along C and the curvature will be approximately constant. A uniform magnetic field would of course drive a circular jet. As β_0 decreases, the curve C expands in both directions, but eventually contracts in the y-direction becoming very pointed. This is also understandable, as low β_0 corresponds to a weak deflecting action and an initially horizontal jet will remain horizontal until it is so close to the vertical line current that $\boldsymbol{B}_1$ becomes very large.

We are now in a position to estimate the validity of our neglect of the path-integral term in (8.8). Suppose that β_0 is small and that far from the driving current the arriving and departing jets are separated by a distance a. The neglect of the field due to the current I_2 in the jet compared to that due to I_1 is valid provided

$$\frac{I_2}{a} \ll \frac{I_1}{x}. \tag{8.13}$$

This clearly breaks down for x sufficiently large. Thus, we should be suspicious of solutions that follow the entirety of the curves in figure 13 when β_0 is small, even when $I_2 \ll I_1$. When $I_2 \sim I_1$, the solutions we have found will break down when x is as large as some characteristic dimension of C.

When all of the terms in (8.8) are of the same order, it must, in general, be solved iteratively, because of the path-integral term which links the local properties of C to those of the entire curve. The solutions will tend to be highly dependent on the particular portion of the circuit C which is held fixed in space and are thus difficult to discuss in general. A natural case to consider is one where the fixed return path of the current I_2 occurs at infinity. Then (8.8) applies over all of C, which will not now be closed. One would expect the jet to straighten out at large distances from I_1, and indeed, this must occur. The equilibrium condition (8.8) enables us to calculate the

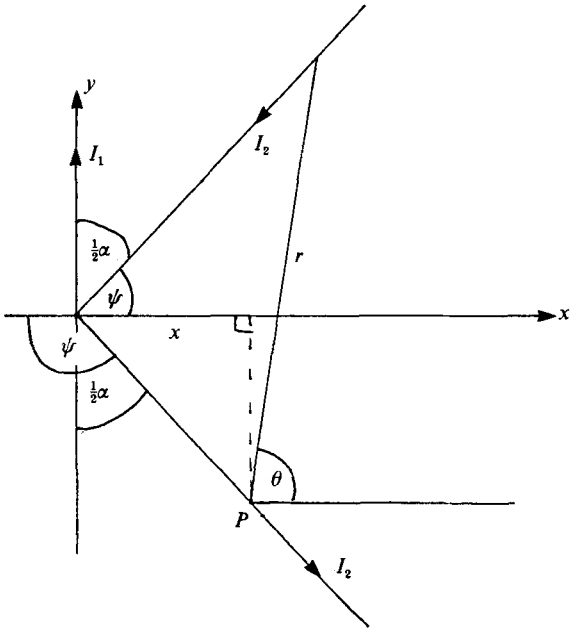

FIGURE 14. Asymptotic equilibrium of current-carrying jet. The field at P due to I_1 and I_2 must cancel.

total angle of deflection, α, between the two asymptotes of C. For large x, the change in $\theta(s)$ over the curved portion of C is small. The line integral is therefore dominated by the contribution from the straight portions of the jet, and the configuration is asymptotically equivalent to that of two line currents inclined at $\frac{1}{2}\alpha$ to the vertical, as in figure 14. (If the angles of inclination are not the same then it is impossible for both the inclined line currents to be in equilibrium.) Thus for large x, (8.8) reduces to

$$2\frac{I_1}{I_2} = x\oint\frac{\mathrm{d}\theta}{r}, \tag{8.14}$$

or from figure 14

$$2\frac{I_1}{I_2} = x\int_{\frac{1}{2}\pi-\frac{1}{2}\alpha}^{\frac{1}{2}\pi+\frac{1}{2}\alpha}\frac{\mathrm{d}\theta}{r} = x\int_{\frac{1}{2}\pi-\frac{1}{2}\alpha}^{\frac{1}{2}\pi+\frac{1}{2}\alpha}\frac{\mathrm{d}\theta}{\sin\alpha}\frac{\sin(\theta-\frac{1}{2}\pi+\frac{1}{2}\alpha)}{(x/\sin\frac{1}{2}\alpha)}, \tag{8.15}$$

and so

$$\cos\tfrac{1}{2}\alpha = \left[1+\left(\frac{I_1}{I_2}\right)^2\right]^{-\frac{1}{2}}. \tag{8.16}$$

For the case of equal currents I_1 and I_2, This gives a total angle of deflection $\alpha = 131°$. Unlike the case of §§2–4, this value is independent of the physical parameters, coming as it does from a geometrical constraint for equilibrium at infinity, rather than an integrated effect along the jet.

The above theoretical results can be extended to different geometries, and even to imperfectly linked a.c. circuits with an unknown mutual inductance. There are, however, some problems in conducting experiments with the configuration discussed in this section, due to the difficulty of ensuring good behaviour of the circuit of which the liquid metal forms part. It is well known that 'sausage' and 'spiral' instabilities can occur in current-carrying fluid jets (e.g. Shercliff 1965). Should such an

instability occur, the cross-sectional area of the jet would diminish in places until the jet broke up, at which point the circuit C would be broken. The associated sudden change of force would lead to chaotic and undesirable behaviour of the jet. We therefore conclude this section with a brief discussion on the stability of a current-carrying jet.

A full stability analysis must take into account the curvature of the jet path C, the effects of the transverse magnetic field B_1, and the non-uniform distribution of a.c. currents. These present formidable difficulties. However, it seems reasonable to expect that the stability behaviour will be qualitatively similar to that of a cylindrical jet carrying a uniform current. This has been extensively analysed by Murty (1960) and Gupta (1964). The effect of the current is destabilizing, while the presence of surface tension ensures the existence of a maximal growth rate for any disturbance. The timescale t_0 on which the fastest mode grows is given approximately by

$$t_0 = \frac{2\pi d_0^2}{I_2}\left[\frac{2\rho}{\mu_0}\right]^{\frac{1}{2}}. \tag{8.17}$$

Now the time taken for the jet to be deflected through an angle α along a path of typical curvature K_0, t_1, is given by

$$t_1 = \frac{\alpha}{K_0 u_0}. \tag{8.18}$$

If $t_1 < t_0$, then any disturbance will be advected downstream before it has time to grow and we expect the jet to be stable. From (8.17), (8.18) and (8.3)

$$\frac{t_0}{t_1} = \frac{2\sqrt{2}}{\alpha}\frac{B_0/(\mu_0\rho)^{\frac{1}{2}}}{u_0}, \tag{8.19}$$

where B_0 is a typical value of B_1+B_2. Envisaging a possible experiment with mercury, we take the values $B_0 = 0.1$ T, $u_0 = 1$ m/s, $\alpha = 30°$ and $\rho = 1.36\times10^4$ kg/m^3. We find

$$\frac{t_0}{t_1} = 4.13. \tag{8.20}$$

Thus it seems that deflection of a metal jet in the manner discussed in this section will be possible, although it is clear that the process is perilously close to instability. Stability considerations are therefore likely to restrict the scope of potential applications.

9. Concluding remarks

In this paper we have investigated two mechanisms by which the ultimate position of a stream of conducting fluid may be controlled. Although the fluid-dynamical techniques we have used are elementary, they do seem to give a reasonable description of the real behaviour, as witnessed by experiment.

The use of electromagnetic fields as controlling devices in the metallurgical industry is growing. Liquid metal may be stirred, heated and shaped without resort to mechanical means. Usually the fluid flow that results is complex in nature, and is often turbulent. Here, by contrast, the flow is particularly simple and yet fairly realistic, which increases the practical value of the process. The analysis is fairly general and may be extended to cover particular geometries of industrial interest.

Interesting analogies can be drawn between the magnetohydrodynamic problems we have considered and parallel ones in hydrodynamics. For example, let the half-

space $x < 0$ consist of fluid and consider the effect of a line vortex at $x = -L, y = 0$. The deformation of the free surface $x = 0$ will then be identical in form to that given in (3.6). Compared to the problem studied in this paper, dynamic pressure along the surface streamline replaces the magnetic pressure, while surface tension mirrors the momentum flux of the metal jet. Although the surface tension is of opposite sign to the momentum flux, its effect in the hydrodynamic problem is mathematically equivalent because there the fluid lies on the opposite side of $x = 0$, and the appropriate value of the surface curvature is negative.

There are also similarities between the analysis of §8 and calculations involving line vortices, although the parallel here is less exact because of the differing conditions for equilibrium. Thus, a similar equation to (8.6) may be found in Batchelor (1967, p. 509).

The authors would like to gratefully acknowledge the support of CNRS, ALCOA and the hospitality of Madylam during the preparation of this paper.

Note added in proof. It has been pointed out by M. D. Cowley, to whom the authors are grateful for this and other comments, that the argument leading to expression (5.1) is erroneous. In fact, the unmodified magnetic pressure, p_M, is at least as accurate as (5.1) when δ/d_0 is small but not negligible, However, the percentage difference between these two expressions is significantly smaller than the experimental uncertainty, and thus the results of this paper are not affected by this oversight.

REFERENCES

BATCHELOR, G. K. 1967 *An Introduction to Fluid Dynamics*. Cambridge University Press.

ELLIOTT, R. S. 1966 *Electromagnetics*, p. 314. McGraw-Hill.

ETAY, J. 1980 Formage et guidage des métaux liquides sous l'action de champs magnétiques alternatifs. *Report de D.E.A. de Mécaniques des Fluides, Inst. Natn. Polytechnique, Grenoble.*

ETAY, J. & GARNIER, M. 1982 Le contrôle electromagnétique des surfaces métalliques liquides et ses applications. *J. Méch. Theor. Appl.* **1**, 911–925.

GUPTA, A. S. 1964 On the capillary instability of a jet carrying an axial current with or without a longitudinal magnetic field. *Proc. R. Soc. Lond.* A **278**, 214–227.

MESTEL, A. J. 1982 Magnetic levitation of liquid metals. *J. Fluid Mech.* **117**, 27–43.

MESTEL, A. J. 1984 On the flow in a channel induction furnace. *J. Fluid Mech.* **147**, 431–447.

MURTY, G. S. 1960 Instability of a conducting fluid cylinder due to an axial current. *Arkiv Fysik* **18**, 241–249.

RAYLEIGH, J. W. S. 1894 *Theory of Sound*. Macmillan.

SHERCLIFF, J. A. 1965 *A Textbook of Magnetohydrodynamics*. Pergamon.

SHERCLIFF, J. A. 1981 Magnetic shaping of molten metal columns. *Proc. R. Soc. Lond.* A **375**, 455–473.

SNEYD, A. D. & MOFFATT, H. K. 1982 The fluid dynamics of the process of levitation melting. *J. Fluid Mech.* **117**, 45–70.

THOMPSON, W. B. 1962 *An Introduction to Plasma Physics*. Pergamon.